HHS Public Access

Author manuscript

Nanotoxicology. Author manuscript; available in PMC 2019 March 12.

Published in final edited form as:

Nanotoxicology. 2018 March ; 12(2): 153–168. doi:10.1080/17435390.2018.1425501.

Macrophage polarization and activation at the interface of multi-walled carbon nanotube-induced pulmonary inflammation and fibrosis

Jie Dong and **Qiang Ma**

Receptor Biology Laboratory, Toxicology and Molecular Biology Branch, Health Effects Laboratory Division, National Institute for Occupational Safety and Health, Centers for Disease Control and Prevention, Morgantown, WV, USA

Abstract

Pulmonary exposure to carbon nanotubes (CNTs) induces fibrosing lesions in the lungs that manifest rapid-onset inflammatory and fibrotic responses, leading to chronic fibrosis in animals and health concerns in exposed humans. The mechanisms underlying CNT-induced fibrogenic effects remain undefined. Macrophages are known to play important roles in immune regulation and fibrosis development through their distinct subsets. Here we investigated macrophage polarization and activation in mouse lungs exposed to multi-walled CNTs (MWCNTs). Male C57BL/6J mice were treated with MWCNTs (XNRI MWNT-7) at 40 μg per mouse (~1.86 mg/kg body weight) by oropharyngeal aspiration. The treatment stimulated prominent acute inflammatory and fibrotic responses. Moreover, it induced pronounced enrichment and polarization of macrophages with significantly increased M1 and M2 populations in a time-dependent manner. Induction of M1 polarization was apparent on day 1 with a peak on day 3, but declined rapidly thereafter. On the other hand, the M2 polarization was induced on day 1 modestly, but was remarkably elevated on day 3 and maintained at a high level through day 7. M1 and M2 macrophages were functionally activated by MWCNTs as indicated by the expression of their distinctive functional markers, such as iNOS and ARG1, with time courses parallel to M1 and M2 polarization, respectively. Molecular analysis revealed MWCNTs boosted specific STAT and IRF signaling pathways to regulate M1 and M2 polarization in the lungs. These findings suggest a new mechanistic connection between inflammation and fibrosis induced by MWCNTs through the polarization and activation of macrophages during MWCNT-induced lung pathologic response.

CONTACT Qiang Ma, qam1@cdc.gov, Mailstop 3014, 1095 Willowdale Road, Morgantown, WV 26505, USA.

Supplemental data for this article can be accessed here.

Disclosure statement

The authors declare there are no competing financial interests.

The findings and conclusions in this report are those of the authors and do not necessarily represent the views of the National Institute for Occupational Safety and Health.

Keywords

M1–M2 polarization; multi-walled carbon nanotube; macrophage; inflammation; fibrosis

Introduction

Pulmonary inflammation and fibrosis are the most predominant pathological effects induced by carbon nanotubes (CNTs) in experimental animals (Donaldson et al. 2006; Dong and Ma 2015). Field studies have revealed significant induction and accumulation of inflammatory and fibrotic mediators and biomarkers in the body fluids of workers exposed to CNTs through respiration, implying a similar adverse health impact of CNT exposure in humans (Fatkhutdinova et al. 2016; Liou et al. 2015). These findings, along with the rapid expansion in the production and application of CNTs in industrial and consumer products, have raised considerable concerns over the potential pathological effects of CNTs and CNT-containing products on humans in recent years (De Volder et al. 2013; Donaldson et al. 2006; Dong and Ma 2015; Kumar et al. 2017; Schulte et al. 2012).

CNTs, including single-walled carbon nanotubes (SWCNTs) and multi-walled carbon nanotubes (MWCNTs), possess unique physicochemical properties, such as a nano-scaled size, a fiber-like shape(i.e. high aspect ratio), and strong carbon–carbon bonds through sp^2 hybridization, which confer CNTs high respirability, poor solubility, and substantial biopersistence to degradation in biological systems. It is believed that these features make many types of CNTs to behave like inflammatogenic and fibrogenic foreign bodies, such as asbestos and silica, to cause inflammation, fibrosis, and malignancy in the lungs. Indeed, pathological analysis from a large number of animal studies demonstrates that CNTs potently induce rapid-onset inflammatory and fibrotic responses that may lead to chronic fibrosis in the lungs (Aiso et al. 2010; Dong and Ma 2016c; Dong et al. 2015; Lam et al. 2004; Mangum et al. 2006; Muller et al. 2005; Park et al. 2011; Porter et al. 2010; Reddy et al. 2012; Shvedova et al. 2005; Vietti, Lison, and van den Brule 2016; Warheit et al. 2004). In these observations, pronounced acute inflammation often proceeds chronic fibrotic lesions, suggesting an interplay between inflammation and tissue fibrosis in the biphasic development of lung fibrosis (Dong and Ma 2015, 2016b). The mechanism(s) by which CNTs stimulate the inflammatory and fibrotic responses and how the interactions between them determine chronic outcomes in the lungs remain poorly understood.

The pulmonary inflammation following foreign body deposition and epithelial damage commonly initiates with the infiltration, accumulation, and activation of inflammatory cells, such as neutrophils, macrophages, and T and B lymphocytes, to orchestrate the clearance of foreign bodies, tissue debridement, and tissue repair in a time-dependent fashion. A failure or overzealous function of these cells would compromise tissue integrity and function leading to various acute and chronic pathologic conditions including fibrosis (Borthwick, Wynn, and Fisher 2013; Wynn and Barron 2010). Among the cells, lung macrophages, including infiltrated monocytes and resident macrophages, have been recognized as major mediators of many functions that include, in addition to engulfing, digesting, and transporting the foreign bodies directly, the secretion of an array of soluble cytokines,

chemokines, and growth factors, such as TNF-α, IL-1 α, IL-1β, IL-6, MCP-1, TGF-β1, and PDGF, to regulate inflammation, tissue repair, and immune functions. Moreover, recent studies have highlighted the importance of specific subsets or polarization states of macrophages, in particular, the M1 (classically activated or polarized) and M2 (alternatively activated or polarized) macrophages, in maintaining tissue homeostasis and promoting disease development. For instance, in the case of parasitic infection with parasite egg deposition, macrophages are shown to undertake an M2 polarization under the influence of type 2 T helper (Th2) cells. The M2 macrophages then promote the development of granulomatous fibrosis by provoking an anti-inflammatory but pro-fibrotic environment rich in pro-fibrotic cytokines and growth factors. These mediators inhibit M1 macrophage-mediated inflammatory reactions, but activate fibroblasts and myofibroblasts to produce and deposit copious amounts of fibrotic extra-cellular matrix (ECM) proteins and form granulomatous foci around deposited eggs, which is defined as a type 2 response (Wynn and Barron 2010).

Whether CNTs elicit M1–M2 polarization and response to modulate inflammation and fibrosis is an intriguing question for understanding CNT-induced lung pathology, but supporting evidence, in particular, the *in vivo* data regarding fibrosis development, is lacking. By using an unbiased array approach, we recently found that a Th2-driven immune response was significantly enriched in MWCNT-exposed mouse lungs *in vivo*, evidenced by the induced expression of Th2 cytokines, IL-4 and IL-13, and a panel of Th2 signature downstream target genes, including Il4i1, Chia, and Ccl11/Eotaxin (Dong and Ma 2016a). Maximal induction of Th2 genes took place on day 7 post-exposure, at which time acute inflammation reaches a peak but subsides rapidly thereafter, whereas the pathologic phenotype transits to chronic fibrosis, supporting a role of Th2 functions in the chronic progression of fibrosis. Induction of Th2 cytokines occurred in CD4+ T lymphocytes, indicating the activation of Th2 cells. Mechanistically, activation of the Th2-type response by MWCNTs was mediated by the activation of the IL-4Ra/STAT6 signaling pathway, as revealed by an increased level of phosphorylated STAT6 and up-regulated expression of GATA-3, the transcription factor controlling the expression of Th2 target genes, in CD4+ T cells. These findings suggest a molecular connection between acute inflammation and fibrosis development induced by MWCNT exposure via a Th2 response. IL-4 and IL-13 have been shown to function as potent pro-fibrotic mediators to drive fibrosis in a variety of fibrotic diseases and animal models (Wynn, 2015). In these cases, M2 macrophage polarization and response constitute the major innate immune arm of the Th2 response.

In light of the much anticipated role of M2 macrophages in fibrosis development and the evidence of Th2 induction at the transition from acute inflammation to chronic fibrosis in CNT-exposed lungs, we posited that CNTs stimulate the M1–M2 polarization of macrophages in exposed lungs to regulate the initiation and resolution of acute inflammation and the progression of fibrosis. In this study, we analyzed the dynamic phenotypic and functional changes of macrophages in MWCNT-exposed mouse lungs that are consistent with macrophage polarization and activation. The results reveal that M1–M2 immune responses were remarkably induced in the early phase response to MWCNT exposure in the lungs, supporting an M1 and M2 paradigm of macrophage activation as a novel molecular mechanism to initiate and promote CNT-induced acute and chronic lung lesions.

Materials and methods

Multi-walled carbon nanotubes

The MWCNTs used in this study were obtained from Mitsui & Company (XNRI MWNT-7, lot #0507 2001K28, Tokyo, Japan). This lot was fully characterized and described in previous reports, in which acute, subchronic, and chronic exposures were conducted (Dong and Ma 2017a; Dong et al. 2015; Porter et al. 2010). The MWCNTs have an average surface area of 26 m^2/g as measured by nitrogen absorption–desorption technique. The length distribution is log normal with a median length of 3.86 μm and a geometric SD of 1.94, whereas the width distribution follows normal distribution with a count mean diameter of 49 nm and a SD of 13.4, as determined by scanning electron microscopy when suspended in a dispersion medium (DM). Trace element contaminations were low, with 0.78% for all metals, 0.41% for sodium, and 0.32% for iron. The lipopolysaccharides (LPS)/endotoxin level of the MWCNT preparation was examined and was found to be below the level of detection.

DM was used to disperse MWCNTs. DM containing Ca^{2+}- and Mg^{2+}-free phosphate-buffered saline (PBS), pH 7.4, 0.6 mg/ml mouse serum albumin (Sigma-Aldrich, St. Louis, MO) and 0.01 mg/ml 1,2-dipalmitoyl-sn-glycerol-3-phosphocholine (Sigma-Aldrich) was freshly prepared before being used to suspend MWCNTs or to serve as vehicle control for animal treatment. MWCNTs were dispersed in DM via a two-step sonication procedure immediately before use. DM effectively disperses MWCNTs as shown by transmission electron microscopy (Porter et al. 2010). The DM preparation does not cause toxicity or mask the reactivity of MWCNTs at the dose used in this study (Dong and Ma 2016c).

Animals and treatment

Eight- to 10-week-old, specific pathogen-free wild-type (WT) C57BL/6J male mice were purchased from The Jackson Laboratory (Bar Harbor, ME). Mice were maintained in an accredited, specific pathogen-free, and environmentally controlled facility at the National Institute for Occupational Safety and Health. All animal experiments were performed in accordance with the guidelines of the Animal Care and Use Committee (ACUC). A single dose of 50 μl of DM or 50 μl of MWCNT suspension containing 40 μg of MWCNTs (approximately 1.86 mg/kg body weight) was administered by oropharyngeal aspiration following an established procedure described previously (Porter et al. 2010). The use of the 40 lg per mouse dose was based on previous dose–response studies, in which MWCNTs at this dose induced significant inflammation and fibrosis in mouse lungs; moreover, this dose has been shown to be relevant to human exposures at workplace (Dong and Ma 2017a). Mouse body weights were recorded and there was no significant difference in the initial body weights among treatment groups. Mice were monitored for general health and toxicity daily after treatment. No apparent effects from treatment were observed during exposure.

Histopathology

Cryostat sections from frozen lung tissues (left lung lobe, 7 μm) were prepared and used. Collagen fibers were determined using the Sirius Red/Fast Green Collagen Staining Kit (Chondrex, Redmond, WA). Sirius Red specifically binds the $[Gly\text{-}X\text{-}Y]_n$ helical structure of

fibrillar collagens, regardless of collagen type. Fast Green binds to non-collagenous proteins to show the tissue structure of the lungs.

Immunohistochemistry and immunofluorescence

Formalin-fixed, paraffin-embedded lung tissue sections (left lung lobe, 5 μm) were deparaffinized, antigen-unmasked, and used to perform immunohistochemistry, following procedures described previously (Dong and Ma 2017a, 2017b, Dong et al. 2016). The primary antibodies used were anti-F4/80 (Bio-Rad/AbD Serotec, Hercules, CA), anti-CD68 (Bio-Rad/AbD Serotec), anti-FIZZ1 (Abcam, Cambridge, MA), anti-YM1 (R&D Systems, Minneapolis, MN), anti-IRF5 (Abcam), and anti-IRF4 (Santa Cruz, Dallas, TX) antibodies. Images were photographed using Olympus Provis AX-70 system (Olympus, Center Valley, PA). Cells with positive staining were counted using the ImageJ program (National Institutes of Health, Bethesda, MD) on microscopic images taken under 20× magnification and presented as the mean ± SD with $n = 4$.

Cryostat sections from frozen lung tissues (left lung lobe, 7 μm) were fixed with 4% paraformalde-hyde and used for immunofluorescence staining, following procedures described previously (Dong and Ma 2017a, 2017b). The primary antibodies used were anti-Collagen I (Abcam), anti-F4/80 (Abcam), anti-CD86 (Santa Cruz), anti-CD206 (Abcam), anti-iNOS (Santa Cruz), anti-ARG1 (Abcam), anti-phospho-STAT1 (Tyr701, Cell Signaling Technology, Danvers, MA), and anti-phospho-STAT6 (Y641, Abcam) antibodies. Images were taken with a Zeiss LSM 780 confocal microscope (Carl Zeiss Microscopy, Jena, Germany). Cells with positive staining were counted using the ImageJ program on microscopic images taken under 40× magnification and presented as the mean ± SD ($n = 4$).

Quantitative RT-PCR (qRT-PCR)

Total RNA was extracted from mouse lungs using RNeasy Mini Kit (QIAGEN, Valencia, CA). cDNA was produced with QuantiTect Reverse Transcription system (QIAGEN), and used for real-time PCR analysis with RT^2 SYBR Green ROX qPCR Mastermix (QIAGEN) and ABI Sequence Detection System 7500 (Thermo Fisher Scientific, Waltham, MA), as described previously (Dong et al. 2015). Mouse housekeeping gene glyceraldehyde 3-phosphate dehydrogenase (Gapdh) was used as an internal control for normalization. Primer sequences are as follows: Fizz1-forward: 5′-CTGCCCTGCTGGGATGACT-3′, Fizz1-reverse: 5′-CATCATATCAAAGCTGGGTTCTCC-3′, Ym1-forward: 5′-CAAGTTGAAGGCTCAGTGGCTC-3′, Ym1-reverse: 5′-CAAATCATTGTGTAAAGCTCCTCTC-3′, Gapdh-forward: 5′-ACTGGCATGGCCTTCCG-3′, and Gapdh-reverse: 5′-CAGGCGGCACGTCAGATC-3′. Fold changes were presented as the mean ± SD ($n = 5$).

Immunoblotting

Randomly selected lung tissue samples were homogenized and lysed in T-PER Tissue Protein Extraction Reagent (Thermo Fisher Scientific). Whole protein extract (20 μg) was resolved on a 4–15% or 8–16% Criterion TGX Gel (Bio-Rad). Representative blotting images were presented, with Actin as control. The primary antibodies used were anti-CD86 (Boster, Pleasanton, CA), anti-MHC II (Thermo Fisher Scientific-eBioscience), anti-CD206

(Abcam), anti-CD163 (Abcam), anti-iNOS (Santa Cruz), anti-ARG1 (Santa Cruz), anti-FIZZ1 (Abcam), anti-YM1 (R&D Systems), anti-phospho-STAT1 (Tyr701, Cell Signaling Technology), anti-STAT1 (Cell Signaling Technology), anti-phospho-STAT6 (Y641, Abcam), anti-STAT6 (Cell Signaling Technology), anti-phospho-STAT3 (Tyr705, Cell Signaling Technology), anti-STAT3 (Cell Signaling Technology), anti-IRF5 (Abcam), anti-IRF4 (Proteintech, Rosemont, IL), and anti-Actin (Santa Cruz) antibodies.

Statistical analysis

Statistical analyses of differences between experimental groups were performed using one-way ANOVA followed by between group comparisons using standard procedures. The representative data were presented as the mean ± SD. A p value of less than 0.05 was considered statistically significant (*$p < 0.05$, **$p < 0.01$, and ***$p < 0.001$). The statistical significance between experimental groups was further examined by post-hoc Tukey HSD (Honestly Significant Difference) test, and consistent results were obtained.

Results

Macrophage enrichment and infiltration in the early phase response to MWCNT exposure

The early phase pulmonary response to MWCNTs leading to chronic fibrosis is characterized by acute inflammation and rapid-onset fibrotic changes before progression to the chronic stage (Dong and Ma 2017a; Dong et al. 2015). This dynamic, biphasic development of fibrosis implicates a role of innate immune/inflammatory functions in the transition from an acute response to chronic fibrosis in CNT-exposed lungs (Dong and Ma 2016a). Given the critical role of macrophages in both innate immune regulation and fibrosis, we focused our analysis on the dynamic changes of macrophages during the early phase response induced by MWCNT exposure. For this purpose, we chose day 1, day 3, and day 7 post-exposure as the time points to represent the immediate, intermediate, and peak stages of the early phase response for the study.

Mice were exposed to a single dose of DM, the vehicle control, or MWCNTs (40 μg/mouse) by oropharyngeal aspiration. Sirius Red collagen staining showed that fibrillar collagens were dramatically induced by MWCNTs with increasing amounts deposited in lung interstitial tissues from day 1 to day 7 post-exposure, forming varying sizes of fibrotic foci around MWCNT deposits (Figure 1(A) and Supplementary Figure S1). Double immunofluorescence staining revealed that, within the fibrotic foci, F4/80+ macrophages were remarkably enriched, interspersing among significantly increased and condensed Collagen I fibers (Figure 1(B)). The overall population of macrophages was assessed by detecting two commonly used pan macrophage surface markers, F4/80, which is encoded by the gene Emr1 and is expressed on most tissue macrophages in mice, and CD68, which is encoded by the gene Cd68 and is expressed on all macrophages (Murray and Wynn 2011). Immunohistochemistry clearly showed that F4/80+ cells (Figure 1(C), left panel) and CD68+ cells (Figure 1(D), left panel) were dramatically increased in the interstitial, perivascular, and peribronchial regions in MWCNT-exposed lungs, compared with the control, during the early phase response to MWCNTs. Induction of F4/80+ cells (Figure 1(C), right panel) or CD68+ cells (Figure 1(D), right panel) by MWCNTs was statistically

significant at all the time points examined, with a significantly higher induction on day 3 compared with that on day 1 post-exposure, indicating that MWCNT exposure rapidly and dramatically induces the enrichment and infiltration of macrophages in the lungs.

Phenotypic characterization of M1 and M2 polarization induced by MWCNTs

In response to environmental cues in tissues, both bone marrow-derived monocytes and tissue resident macrophages may differentiate into M1 and M2 macrophages with distinct phenotypes to mediate specific functions. To examine whether M1–M2 macrophage polarization takes place in MWCNT-induced pulmonary pathology, a number of surface markers for M1 and M2 macrophages were analyzed. By immunoblotting analysis, we found that the expression of CD86 (B7–2) and MHC II (major histocompatibility complex II), two surface markers for M1 phenotype, was induced in lung tissues on day 1 and day 3, but not day 7, post-exposure to MWCNTs; whereas the expression of CD206 (mannose receptor C-type 1 or MRC1) and CD163 (hemoglobin scavenger receptor), two surface markers for M2 phenotype, was induced on day 1 only slightly, but was remarkably elevated in lung tissues on day 3 and day 7, post-exposure to MWCNTs (Figure 2(A)). These results suggest that MWCNT exposure elicits macrophage polarization in the lungs, with M1 polarization occurring more rapidly than M2 polarization.

Double immunofluorescence staining was performed to further ascertain the differentiation of M1 and M2 macrophages. In MWCNT-exposed lungs, the number of M1 macrophages (CD68+ F4/80+) was significantly increased at all the time points detected in comparison with control, with high levels of induction on day 1 and day 3, but significantly reduced level on day 7 (Figure 2(B) and Supplementary Figure S2(A)). Induction of M2 macrophages (CD206+ F4/80+) exhibited a different time course from that of M1, in which M2 macrophages continuously increased in numbers from day 1 to day 7 post-exposure, with the changes between day 1 and day 3 and between day 3 and day 7 statistically significant (Figure 2(C) and Supplementary Figure S2(B)). These results visualized the enrichment of M1 and M2 macrophages induced by MWCNTs in the lungs. Moreover, the findings revealed overlapping but distinct time courses of M1 and M2 induction, which are reflective of the highly dynamic early phase pathologic changes and are consistent with the distinctive functions of M1 and M2 macrophages in inflammation and fibrosis development.

Functional activation of M1 and M2 macrophages in MWCNT-exposed lungs

Upon activation, M1 macrophages express a high level of inducible nitric oxide synthase (iNOS or NOS2) that catalyzes the production of nitric oxide (NO), a key mediator of the killing function of M1 cells; on the other hand, M2 macrophages use arginase 1 (ARG1) to convert L-arginine to L-ornithine and polyamines that, in part, mediate the repair function of M2 macrophages. Therefore, the induction of iNOS and ARG1 is often used as indicators for activation of M1 and M2 macrophages, respectively (Roszer, 2015). In MWCNT-exposed lungs, iNOS protein was induced, as revealed by immunoblotting, at all the time points detected, with a slight induction on day 1, but a remarkable elevation to a peak level on day 3, followed by reduction on day 7 (Figure 3(A)). The expression of ARG1 protein was slightly induced on day 1, but was dramatically induced on day 3 and further increased to a higher level on day 7 post-exposure (Figure 3(A)). Therefore, the induction of iNOS and

ARG1 by MWCNTs correlates well with the induction of M1 and M2 polarization, respectively, indicating the functional activation of M1 and M2 macrophages.

To further corroborate the activation of M1 and M2 macrophages, double immunofluorescence staining was performed. MWCNT exposure significantly increased the number of iNOS+ F4/80+ cells, i.e. activated M1 macrophages, compared with control, at all the time points detected, with a slightly increased level on day 1, a peak level on day 3, and a reduced induction on day 7; the changes between day 1 and day 3 and between day 3 and day 7 were statistically significant (Figure 3(B) and Supplementary Figure S3(A)). The number of ARG1+ F4/80+ cells, i.e. activated M2 macrophages, was slightly increased with a statistical significance on day 1, but was distinctly elevated on day 3 and day 7, by MWCNTs; the change between day 1 and day 3 was statistically significant (Figure 3(C) and Supplementary Figure S3(B)). These results are in a good agreement with the findings from immunoblotting (Figure 3(A)), demonstrating the distinctive functional activation of M1 and M2 macrophages in MWCNT-stimulated inflammation and fibrosis.

M2 macrophages are known to play a critical role in fibrosis development. Therefore, we further analyzed the activation of M2 macrophages in MWCNT-induced lung fibrosis by examining the levels of two additional marker proteins of mouse M2 macrophages with pro-fibrotic functions, FIZZ1 (found in inflammatory zone 1; resistin-like molecule a or RELM-α; resistin-like-α or RETNL-α) and YM1 (chitinase 3-like 3 or CHI3L3; eosinophil chemotactic factor-lymphocyte or ECF-L) (Raes et al. 2002; Roszer, 2015). MWCNTs significantly induced the mRNA expression of Fizz1 and Ym1 in mouse lungs on days 1, 3, and 7 post-exposure, with a peak on day 7 (Figure 4(A)). Moreover, the protein levels of FIZZ1 and YM1 were dramatically elevated by MWCNTs at all the time points detected, with a continuously increased induction from day 1 to day 7 (Figure 4(B)). Immunohistochemistry demonstrated that the numbers of FIZZ1+ cells (Figure 4(C), left panel) and YM1+ cells (Figure 4(D), left panel) were remarkably increased in MWCNT-exposed lungs during the early phase response to MWCNTs. The increase of the number of FIZZ1+ cells (Figure 4(C), right panel) or YM1+ cells (Figure 4(D), right panel) by MWCNTs was statistically significant, compared with control, at all the time points detected; induction on day 3 was statistically significant compared with that on day 1, for both proteins. The increased expression of FIZZ1 and YM1 further confirmed the functional activation of M2 macrophages in the lungs exposed MWCNTs.

Signaling pathways of macrophage polarization and activation in MWCNT-exposed lungs

M1 and M2 polarization is mediated through specific signaling pathways in macrophages (Martinez and Gordon 2014). Activation of STAT1 and IRF5 would promote the M1 polarization to result in pro-inflammatory and cytotoxic M1 functions, whereas activation of STAT6/STAT3 and IRF4 stimulates the M2 polarization to confer anti-inflammatory and tissue repair activities.

To analyze the signaling pathways involved in MWCNT-induced M1–M2 polarization, we first examined phosphorylation of STAT1, STAT6, and STAT3 in lung tissues, which indicates activation of the signaling pathways for these transcription factors. Immunoblotting showed the level of p-STAT1 was moderately increased on day 1 and strikingly elevated on

day 3; but induction was markedly reduced on day 7 post-exposure to MWCNTs (Figure 5(A)). On the other hand, the levels of p-STAT6 and p-STAT3 were slightly increased on day 1 and were remarkably elevated on both day 3 and day 7 post-exposure (Figure 5(A)). Induction of p-STAT1 and p-STAT6 in macrophages was examined by double immunofluorescence staining. In MWCNT-exposed lungs, the number of p-STAT1+ F4/80+ macrophages was significantly increased, compared with control, at all the time points detected, starting from day 1, reaching a peak on day 3, and reducing to a lower level on day 7; the changes between day 1 and day 3 and between day 3 and day 7 were statistically significant (Figure 5(B) and Supplementary Figure S4(A)). In contrast, the number of p-STAT6+ F4/80+ macrophages was slightly increased with a statistical significance on day 1, but was markedly elevated on day 3 and day 7 upon MWCNT exposure; the change between day 1 and day 3 was statistically significant (Figure 5(C) and Supplementary Figure S4(B)). These results are consistent with the findings from immunoblotting (Figure 5(A)). These patterns of activation of M1 and M2 STAT proteins by MWCNTs correlate well with the time courses of M1 and M2 polarization induced by MWCNTs, respectively.

The induction of IRF5 and IRF4 was examined for activation of IRF signaling in MWCNT-exposed lungs. Similar to the time course of p-STAT1 level affected by MWCNTs, IRF5 level was slightly increased on day 1 and dramatically increased on day 3; induction was reduced to an intermediate level on day 7 compared with those on day 1 and day 3 (Figure 6(A)), whereas, IRF4 level was shown to be remarkably increased on day 3 and day 7 post-exposure to MWCNTs (Figure 6(A)). The cells expressing IRF5 or IRF4 were visualized by immunohistochemistry. The number of IRF5+ cells was increased by MWCNTs and the induction was statistically significant, compared with control, at all the time points detected; induction was moderate on day 1, was strikingly increased on day 3, but was reduced on day 7; the changes between day 1 and day 3 and between day 3 and day 7 were statistically significant (Figure 6(B)). On the other hand, the number of IRF4+ cells was increased by MWCNTs on day 3 and day 7 with statistical significance, with statistically significant differences between day 1 and day 3 and between day 3 and day 7, in MWCNT-exposed lungs (Figure 6(C)).

Taken together, specific STAT and IRF signaling pathways were significantly activated during M1–M2 polarization in MWCNT-exposed lungs, which correlate with the time courses of the appearance of M1 and M2 macrophages in MWCNT-exposed lungs, implicating the STAT and IRF signaling pathways in controlling macrophage polarization and functionalization induced by MWCNTs.

Discussion

There is an increasing interest in understanding the health impact of exposure to nanomaterials in workers and populations at large, as recent years have witnessed a rapid expansion in nano-production and the commercial application of nano-products worldwide, accompanied by substantial evidence of adverse health effects from nano-exposure in animal studies (Donaldson et al. 2006; Dong and Ma 2015; Schulte et al. 2012). In this respect, CNT-induced pulmonary fibrosis has received a particular attention, because of its potential severe consequences analogous to those of pneumoconiosis caused by dust exposure. From

an experimental point of view, CNT-elicited lung fibrosis serves as a useful model to analyze how nano-exposure stimulates the initiation and progression of chronic fibrotic lesions in the lungs.

The pulmonary fibrotic response to CNT exposure manifests a biphasic development with pronounced acute inflammation preceding chronic fibrosis progression (Dong and Ma 2016b). Specifically, acute inflammation develops abruptly upon exposure and predominates the lesions during the early phase response, which includes infiltration of inflammatory cells and secretion of an array of cytokines, chemokines, and growth factors, along with increased deposition of collagen fibers in the matrix, for up to 7 days after treatment. Thereafter, the acute lesions are resolved rapidly, followed by progression to chronic interstitial fibrosis with formation of granulomatous fibrotic foci around deposited CNT fibers. These findings suggest a close interplay between inflammation and the fibrotic response in the development of lung fibrosis. We have, therefore, targeted to unravel the cellular and molecular underpinnings that control the transition from acute inflammation to chronic fibrosis. In this study, we characterized the phenotypes of lung macrophages that are markedly increased during the early phase response to MWCNT exposure. We demonstrate that MWCNTs elicit apparent polarization and activation of macrophages in the lungs through specific signaling pathways, thus providing a novel cellular and molecular link at the interphase between pulmonary acute inflammation and chronic fibrosis progression through M1–M2 polarization and function.

The MWCNT-induced macrophage polarization was dichotomous with specific and dynamic time courses. M1 macrophages, marked by increased expression of two M1 surface markers, CD86 and MHC II, were significantly increased on day 1, reached a peak on day 3, but declined on day 7 post-exposure. These macrophages were activated as evidenced by parallel induction and decline of iNOS, which catalyzes the production of NO. These findings are consistent with the functions of M1 macrophages in promoting acute inflammation to kill invading microbes, remove deposited foreign bodies, and, at the same time, cause tissue damage. On the other hand, M2 macrophages showed a marked increase on day 3 and predominated on day 7 post-exposure, evidenced by the up-regulation of M2 surface markers, CD206 and CD163, as well as ARG1 that converts L-arginine to L-ornithine and polyamines critical for the reparative functions of M2 macrophages. This delayed but dramatic induction of M2 polarization after M1 induction correlates well with the decline of acute inflammation and its transition to chronic fibrosis progression, reflecting the M2 functions to inhibit M1-mediated, tissue damaging, acute inflammation, but promote tissue debridement and repair. It is believed that, in the presence of a persistent or repetitive stimulant and/or tissue damage, M2 functions become overzealous and imbalanced, causing the over-activation of fibroblasts and myofibroblasts, excessive deposition of collagenous matrix, and fibrotic remodeling of the normal parenchyma, resulting in organ fibrosis.

The M1–M2 polarization of macrophages can be induced by distinct signaling molecules in a context-dependent manner (Martinez and Gordon 2014; Wynn, 2015). Typical stimuli for M1 polarization are pro-inflammatory molecules, such as IFN-γ, IL-12, IL-23, TNF-α, IL-6, IL-1β, specific chemokines, and antigen presenting molecules. Both MWCNTs and SWCNTs stimulate a rapid induction of IFN-γ on day 1 post-exposure (Park et al. 2009,

2011). MWCNTs also induce the expression and secretion of pro-inflammatory cytokines TNF-α, IL-1β, and IL-6, as well as inflammatory signaling molecules TIMP1 and OPN, in the lungs as early as day 1 after treatment (Dong and Ma 2017a, 2017b; Dong et al. 2015). Given the complex nature of the signaling in acute inflammation, it is likely that many of these factors contribute to the induction of M1 polarization. Known stimuli for M2 macrophage polarization include IL-4, IL-13, immune complex + TLR or IL-1R ligands, IL-10, and glucocorticoids. We have previously reported that MWCNTs stimulate a prominent Th2 response at the junction of transition from acute inflammation to chronic fibrosis in mouse lungs (Dong and Ma 2016a). Th2 cytokines IL-4 and IL-13 are markedly elevated, along with their downstream target genes Il4i1, Chia, and Ccl11/Eotaxin, in a time-dependent manner, with peak induction occurring on day 7 post-exposure. Activated Th2 cells exhibit increased signaling of the STAT6 and GATA-3 pathway to mediate the transcription of Th2 genes. These findings implicate a critical role of Th2 functions in MWCNT-induced M2 polarization. This conclusion does not exclude the possibility that MWCNTs directly stimulate macrophages to induce M1 and/or M2 polarization. In addition, CNTs are known to vary with their physicochemical properties and thereby induce variable phenotypes. Thus, whether CNTs other than the MWCNTs being tested in this study stimulate M1–M2 polarization to modulate fibrotic responses is an intriguing question. In this regard, it has been shown that an oxidized MWCNT preparation interacted with macrophage cells *in vitro* and induced a mixed M1–M2 phenotype wherein the M1 phenotype mimicked the response observed in macrophages exposed to LPS, whereas the M2 phenotype mimicked that of macrophages treated with a mixture of IL-4, IL-10, and IL-13, which are known Th2 cytokines (Meng et al. 2015). However, detailed comparisons among CNTs with contrasting properties for their abilities to induce M1–M2 polarization both *in vitro* and *in vivo* are needed to better understand the mechanism of induction of M1–M2 polarization by different types of CNTs.

The Th2-mediated type 2 immune responses are known to exert protective activities important to the maintenance of tissue homeostasis, including promoting anti-helminth immunity, suppressing Th1-driven autoimmune diseases, neutralizing toxins, and regulating wound healing and tissue regeneration. However, when dysregulated, type 2 immunity boosts the pathogenesis of a range of diseases by inducing complex inflammatory responses (Wynn, 2015). The type 2 cytokines IL-4 and IL-13 have been recognized as major drivers for the development of many allergic and fibrotic disorders wherein the Th2 cells and the IL-4 and/or IL-13-conditioned macrophages (i.e. M2 polarized macrophages) play a central role. In these models, M2 macrophages function as the major effector cells to mediate the innate immune arm of the type 2 immune responses. M2 macrophages also secrete more IL-4, IL-13, and other type 2 cytokines to amplify and propel type 2 responses. Consistent with these notions, the CNT-induced Th2 response coincides well with the polarization and activation of M2 macrophages in CNT-exposed lungs, both arising around day 3 and peaking on day 7 post-exposure. From these observations, it is rational to propose that the Th2 response and M2 polarization induced by CNTs in the lungs are interconnected and mutually promoted, thereby instituting a major mechanism by which the transition from acute inflammation to chronic fibrosis is promoted and propagated. It has been reported that CNTs induced or potentiated Th2-type allergy-like airway responses in a number of mouse models

of asthma. For instance, the rod-like MWCNTs, but not tangled MWCNTs, caused allergic airway inflammation with marked eosinophilia, mucus hypersecretion, airway hyperresponsiveness, and elevated expression of Th2-type cytokines (Rydman et al. 2014). MWCNTs potentiated the airway inflammation, fibrosis, and asthma-like responses in mouse lungs pre-conditioned with house dust mite or ovalbumin, accompanied by elevated levels of type 2 alarmins, cytokines, and cells (Ronzani, Casset, and Pons 2014; Ryman-Rasmussen et al. 2009). MWCNTs also induced airway hyper-sensitivity in mouse lungs, which required IL-33 and a subset of innate helper cells (Beamer et al. 2013). In a separate study, mast cells and the IL-33/ST2 axis, which are important for type 2 alarmin signaling, were shown to mediate MWCNT-induced airway and lung fibrotic changes (Katwa et al. 2012). Therefore, the phenotypes of CNT-induced Th2 response in the lungs may vary with inducers and animal models.

It is known that M2 macrophages consist of several subtypes with overlapping but distinguishable functions. Identification of the subtypes and their specific modes of action in CNT-induced responses is necessary to fully understand CNT-induced and M2-mediated functions in lung fibrosis development in future studies. It is also generally accepted that the M1–M2 paradigm represents a simplistic view of the dynamic changes of macrophage phenotypes and functions during disease development (Murray et al. 2014). Therefore, a spectrum of macrophage phenotypes that include, but not limited to, the M1 and M2 macrophages may be induced by MWCNTs in the lungs to control or modulate the progression of inflammation and fibrosis in a time and context-dependent manner, which requires further investigation.

The signaling behind the effects of M1 and M2 stimuli in macrophages has gained certain clarity in recent years (Martinez and Gordon 2014; Sica and Mantovani 2012; Wang, Liang, and Zen 2014). For instance, activation of STAT1 and IRF5 is believed to promote the M1 polarization by up-regulating the expression of inflammatory mediators that boost pro-inflammatory and cytotoxic M1 functions. On the other hand, activation of STAT6/STAT3 and IRF4 would stimulate the M2 polarization to confer anti-inflammatory and tissue repair activities of M2 cells. We found that MWCNTs elicit significant induction and activation of STAT1 and IRF5 with a peak on day 3, which correlates with the induction of M1 macrophages, thus implicating the STAT1 and IRF5 signaling in CNT-induced M1 polarization. It has been shown that rod-like MWCNTs stimulated exaggerated airway fibrosis in Stat1 knockout mouse lungs, which correlated with elevated levels of TGF-β1 protein and Smad2/3 phosphorylation in the lungs of the knockout mice, suggesting that STAT1 plays a protective role against CNT-induced fibrosis (Duke et al. 2017). This observation is consistent with the current finding on the activation of STAT1 and M1 polarization, which is believed to be pro-inflammatory but suppressive to fibrosis. Induction and activation of STAT6/STAT3 and IRF4 by MWCNTs take place on day 3 and dominate on day 7 post-exposure during the early phase response, which correlates with the induction of M2 polarization, thus supporting a role of STAT6/STAT3 and IRF4 signaling in the induction and function of M2 macrophages. Although detailed elucidation of these signaling pathways awaits further investigation, this study identifies the major factors and their signaling pathways for CNT-elicited M1–M2 polarization in the lungs, thus paving the road for future molecular mechanistic studies.

Supplementary Material

Refer to Web version on PubMed Central for supplementary material.

Funding

This work was funded to Q.M. by the Health Effects Laboratory Division and the Nanotechnology Research Center at National Institute for Occupational Safety and Health, Centers for Disease Control and Prevention, USA. No. 7939050W

References

Aiso S, Yamazaki K, Umeda Y, Asakura M, Kasai T, Takaya M, Toya T, et al. 2010 “Pulmonary Toxicity of Intratracheally Instilled Multiwall Carbon Nanotubes in Male Fischer 344 Rats.” Industrial Health 48:783–795. http://www.ncbi.nlm.nih.gov/pubmed/20616469 [PubMed: 20616469]

Beamer CA, Girtsman TA, Seaver BP, Finsaas KJ, Migliaccio CT, Perry VK, Rottman JB, et al. 2013 “IL-33 Mediates Multi-walled Carbon Nanotube (MWCNT)-induced Airway Hyper-reactivity Via the Mobilization of Innate Helper Cells in the Lung.” Nanotoxicology 7:1070–1081. doi: 10.3109/17435390.2012.702230 [PubMed: 22686327]

Borthwick LA, Wynn TA, and Fisher AJ. 2013 “Cytokine Mediated Tissue Fibrosis.” Biochimica et Biophysica Acta 1832:1049–1060. doi:10.1016/j.bbadis.2012.09.014 [PubMed: 23046809]

De Volder MF, Tawfick SH, Baughman RH, and Hart AJ. 2013 “Carbon Nanotubes: Present and Future Commercial Applications.” Science 339:535–539. doi:10.1126/science.1222453 [PubMed: 23372006]

Donaldson K, Aitken R, Tran L, Stone V, Duffin R, Forrest G, Alexander A, et al. 2006 “Carbon Nanotubes: A Review of their Properties in Relation to Pulmonary Toxicology and Workplace Safety.” Toxicological Science 92:5–22. doi:10.1093/toxsci/kfj130

Dong J, and Ma Q. 2015 “Advances in Mechanisms and Signaling Pathways of Carbon Nanotube Toxicity.” Nanotoxicology 9:658–676. doi:10.3109/17435390.2015.1009187 [PubMed: 25676622]

Dong J, and Ma Q. 2016a “In vivo Activation of a T Helper 2-Driven Innate Immune Response in Lung Fibrosis Induced by Multi-walled Carbon Nanotubes.” Archives of Toxicology 90:2231–2248. doi:10.1007/s00204-016-1711-1 [PubMed: 27106021]

Dong J, and Ma Q. 2016b “Myofibroblasts and Lung Fibrosis Induced by Carbon Nanotube Exposure.” Particle and Fibre Toxicology 13:60. doi:10.1186/s12989-016-0172-2 [PubMed: 27814727]

Dong J, and Ma Q. 2016c “Suppression of Basal and Carbon Nanotube-induced Oxidative Stress, Inflammation and Fibrosis in Mouse Lungs by Nrf2.” Nanotoxicology 10:699–709. doi: 10.3109/17435390.2015.1110758 [PubMed: 26592091]

Dong J, and Ma Q. 2017a “Osteopontin Enhances Multi-walled Carbon Nanotube-triggered Lung Fibrosis by Promoting TGF-beta1 Activation and Myofibroblast Differentiation.” Particle and Fibre Toxicology 14:18 doi:10.1186/s12989-017-0198-0. [PubMed: 28595626]

Dong J, and Ma Q. 2017b “TIMP1 Promotes Multi-walled Carbon Nanotube-induced Lung Fibrosis by Stimulating Fibroblast Activation and Proliferation.” Nanotoxicology 11:41–51. doi: 10.1080/17435390.2016.1262919 [PubMed: 27852133]

Dong J, Porter DW, Batteli LA, Wolfarth MG, Richardson DL, and Ma Q. 2015 “Pathologic and Molecular Profiling of Rapid-onset Fibrosis and Inflammation Induced by Multi-walled Carbon Nanotubes.” Archives of Toxicology 89:621–633. doi:10.1007/s00204-014-1428-y [PubMed: 25510677]

Dong J, Yu X, Porter DW, Battelli LA, Kashon ML, and Ma Q. 2016 “Common and Distinct Mechanisms of Induced Pulmonary Fibrosis by Particulate and Soluble Chemical Fibrogenic Agents.” Archives of Toxicology 90:385–402. doi:10.1007/s00204-015-1589-3 [PubMed: 26345256]

Duke KS, Taylor-Just AJ, Ihrie MD, Shipkowski KA, Thompson EA, Dandley EC, Parsons GN, et al. 2017 “STAT1-dependent and -Independent Pulmonary Allergic and Fibrogenic Responses in Mice After Exposure to Tangled Versus Rod-like Multi-walled Carbon Nanotubes.” Particle and Fibre Toxicology 14:26. doi:10.1186/s12989-017-0207-3 [PubMed: 28716119]

Fatkhutdinova LM, Khaliullin TO, Vasil’Yeva OL, Zalyalov RR, Mustafin IG, Kisin ER, Birch ME, et al. 2016 “Fibrosis Biomarkers in Workers Exposed to MWCNTs.” Toxicology and Applied Pharmacology 299:125–131. doi:10.1016/j.taap.2016.02.016 [PubMed: 26902652]

Katwa P, Wang X, Urankar RN, Podila R, Hilderbrand SC,Fick RB, Rao AM, et al. 2012 “A Carbon Nanotube Toxicity Paradigm Driven by Mast Cells and the IL-(3)(3)/ST(2) Axis.” Small 8:2904–2912. doi:10.1002/smll.201200873 [PubMed: 22777948]

Kumar S, Rani R, Dilbaghi N, Tankeshwar K, and Kim KH. 2017 “Carbon NANotubes: a Novel Material for Multifaceted Applications in Human Healthcare.” Chemical Society Reviews 46:158–196. doi:10.1039/c6cs00517a [PubMed: 27841412]

Lam CW, James JT, McCluskey R, and Hunter RL. 2004 “Pulmonary Toxicity of Single-wall Carbon Nanotubes in mice 7 and 90 days After Intratracheal Instillation.” Toxicological Science 77:126–134. doi:10.1093/toxsci/kfg243

Liou SH, Tsai CS, Pelclova D, Schubauer-Berigan MK, and Schulte PA. 2015 “Assessing the First Wave of Epidemiological Studies of Nanomaterial Workers.” Journal of Nanoparticle Research 17:413. doi:10.1007/s11051-015-3219-7 [PubMed: 26635494]

Mangum JB, Turpin EA, Antao-Menezes A, Cesta MF, Bermudez E, and Bonner JC. 2006 “Single-walled Carbon Nanotube (SWCNT)-induced Interstitial Fibrosis in the Lungs of Rats is Associated with Increased Levels of PDGF mRNA and the Formation of Unique Intercellular Carbon Structures that Bridge Alveolar Macrophages in situ.” Particle and Fibre Toxicology 3:15 https://www.ncbi.nlm.nih.gov/pubmed/17134509 [PubMed: 17134509]

Martinez FO, and Gordon S. 2014 “The M1 and M2 paradigm of macrophage activation: time for reassessment.” F1000Prime Reports 6:13. doi:10.12703/P6-13 [PubMed: 24669294]

Meng J, Li X, Wang C, Guo H, Liu J, and Xu H. 2015 “Carbon Nanotubes Activate Macrophages into a M1/M2 Mixed Status: Recruiting NAÏVE Macrophages and Supporting Angiogenesis.” ACS Applied Materials & Interfaces 7:3180–3188. doi:10.1021/am507649n [PubMed: 25591447]

Muller J, Huaux F, Moreau N, Misson P, Heilier J-F, Delos M, Arras M, et al. 2005 “Respiratory Toxicity of Multi-wall Carbon Nanotubes.” Toxicology and Applied Pharmacology 207:221–231. doi:10.1016/j.taap.2005.01.008 [PubMed: 16129115]

Murray PJ, Allen JE, Biswas SK, Fisher EA, Gilroy DW, Goerdt S, Gordon S, et al. 2014 “Macrophage Activation and Polarization: nomenclature and Experimental Guidelines.” Immunity 41:14–20. doi:10.1016/j.immuni.2014.06.008 [PubMed: 25035950]

Murray PJ, and Wynn TA. 2011 “Protective and Pathogenic Functions of Macrophage Subsets.” Nature Reviews: Immunology 11:723–737. doi:10.1038/nri3073

Park EJ, Cho WS, Jeong J, Yi J, Choi K, and Park K. 2009 “Pro-inflammatory and Potential Allergic Responses Resulting From B Cell Activation in Mice Treated with Multi-walled Carbon Nanotubes by Intratracheal Instillation.” Toxicology 259:113–121. doi:10.1016/j.tox.2009.02.009 [PubMed: 19428951]

Park E-J, Roh J, Kim S-N, Kang M-S, Han Y-A, Kim Y, Hong JT, et al. 2011 “A Single Intratracheal Instillation of Single-walled Carbon Nanotubes Induced Early Lung Fibrosis and Subchronic Tissue Damage in Mice.” Archives of Toxicology 85:1121–1131. doi:10.1007/s00204-011-0655-8 [PubMed: 21472445]

Porter DW, Hubbs AF, Mercer RR, Wu N, Wolfarth MG, Sriram K, Leonard S, et al. 2010 “Mouse Pulmonary Dose- and Time Course-responses Induced by Exposure to Multi-walled Carbon Nanotubes.” Toxicology 269:136–147. doi:10.1016/j.tox.2009.10.017 [PubMed: 19857541]

Raes G, De Baetselier P, Noel W, Beschin A, Brombacher F, and Hassanzadeh Gh G. 2002 “Differential Expression of FIZZ1 and Ym1 in Alternatively Versus Classically Activated Macrophages.” Journal of Leukocyte Biology 71:597–602. https://www.ncbi.nlm.nih.gov/pubmed/11927645 [PubMed: 11927645]

Reddy AR, Reddy YN, Krishna DR, and Himabindu V. 2012 “Pulmonary Toxicity Assessment of Multiwalled Carbon NANOTubes in rats Following Intratracheal Instillation.” Environmental Toxicology 27:211–219. doi:10.1002/tox.20632 [PubMed: 20862737]

Ronzani C, Casset A, and Pons F. 2014 “Exposure to Multi-walled Carbon Nanotubes Results in Aggravation of Airway Inflammation and Remodeling and in Increased Production of Epithelium-derived Innate Cytokines in a Mouse Model of Asthma.” Archives of Toxicology 88:489–499. doi:10.1007/s00204-013-1116-3 [PubMed: 23948970]

Roszer T 2015 “Understanding the MYSterious M2 Macrophage Through Activation Markers and Effector Mechanisms.” Mediators of Inflammation 2015:816460. doi:10.1155/2015/816460 [PubMed: 26089604]

Rydman EM, Ilves M, Koivisto AJ, Kinaret PAS, Fortino V, Savinko TS, Lehto MT, et al. 2014 “Inhalation of Rod-like Carbon Nanotubes Causes Unconventional Allergic Airway Inflammation.” Particle and Fibre Toxicology 11:48. doi:10.1186/s12989-014-0048-2 [PubMed: 25318534]

Ryman-Rasmussen JP, Tewksbury EW, Moss OR, Cesta MF, Wong BA, and Bonner JC. 2009 “Inhaled Multiwalled Carbon Nanotubes Potentiate Airway Fibrosis in Murine Allergic Asthma.” American Journal of Respiratory Cell and Molecular Biology 40:349–358. doi:10.1165/rcmb.2008-0276OC [PubMed: 18787175]

Schulte PA, Kuempel ED, Zumwalde RD, Geraci CL,Schubauer-Berigan MK, Castranova V, Hodson L, et al. 2012 “Focused Actions to Protect Carbon Nanotube Workers.” American Journal of Industrial Medicine 55:395–411. doi:10.1002/ajim.22028 [PubMed: 22392774]

Shvedova AA, Kisin ER, Mercer R, Murray AR, Johnson VJ, Potapovich AI, Tyurina YY, et al. 2005 “Unusual Inflammatory and Fibrogenic Pulmonary Responses to Single-walled Carbon Nanotubes in Mice.” American Journal of Physiology. Lung Cellular and Molecular Physiology 289:L698–L708. doi:10.1152/ajplung.00084.2005 [PubMed: 15951334]

Sica A, and Mantovani A. 2012 “Macrophage Plasticity and Polarization: in vivo Veritas.” The Journal of Clinical Investigation 122:787–795. doi:10.1172/JCI59643 [PubMed: 22378047]

Vietti G, Lison D, and van den Brule S. 2016 “Mechanisms of Lung Fibrosis Induced by Carbon Nanotubes: towards an Adverse Outcome Pathway (AOP).” Particle and Fibre Toxicology 13:11. doi:10.1186/s12989-016-0123-y [PubMed: 26926090]

Wang N, Liang H, and Zen K. 2014 “Molecular Mechanisms that Influence the Macrophage M1–M2 Polarization Balance.” Frontiers in Immunology 5:614. doi:10.3389/fimmu.2014.00614 [PubMed: 25506346]

Warheit DB, Laurence BR, Reed KL, Roach DH, Reynolds GA, and Webb TR. 2004 “Comparative Pulmonary Toxicity Assessment of Single-wall Carbon Nanotubes in Rats.” Toxicological Science 77:117–125. doi:10.1093/toxsci/kfg228

Wynn TA 2015 “Type 2 cytokines: Mechanisms and Therapeutic Strategies.” Nature Reviews: Immunology 15:271–282. doi:10.1038/nri3831

Wynn TA, and Barron L. 2010 “Macrophages: master Regulators of Inflammation and Fibrosis.” Seminars in Liver Disease 30:245–257. doi:10.1055/s-0030-1255354 [PubMed: 20665377]

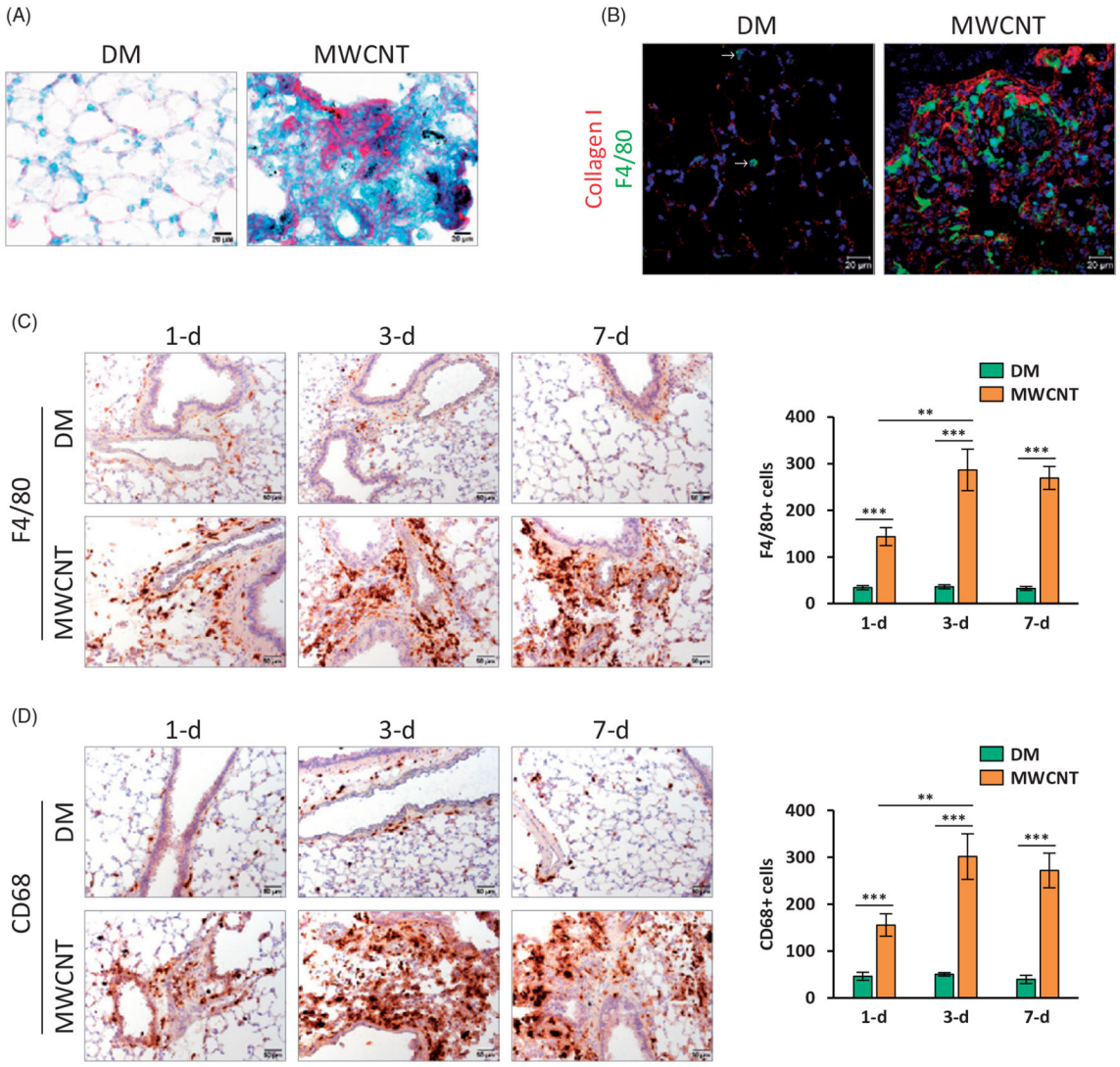

Figure 1.

Lung fibrosis and macrophage enrichment. Wild-type mice treated with DM or MWCNTs (40 μg per mouse) were sacrificed on day 1, 3, or 7 post-exposure. (A) Fibrillar collagens detected by Sirius Red/Fast Green staining in lung tissues from mice exposed for 7 days. Collagen fibers are in red and non-collagenous proteins in green (scale bar: 20 μm). (B) Accumulation of macrophages in fibrotic foci in the lungs on day 7 post-exposure examined by double immunofluorescence staining of F4/80 (green) and Collagen I (red). Blue indicates nuclear staining (scale bar: 20 μm). (C) and (D) Time-dependent induction of macrophages by MWCNTs in the lungs on days 1, 3, and 7 post-exposure determined by immunohistochemistry of F4/80 (C) and CD68 (D). Red indicates positive staining and blue nuclear counterstaining (scale bar: 50 μm). Quantification of positively stained cells is shown as mean ± SD ($n = 4$).

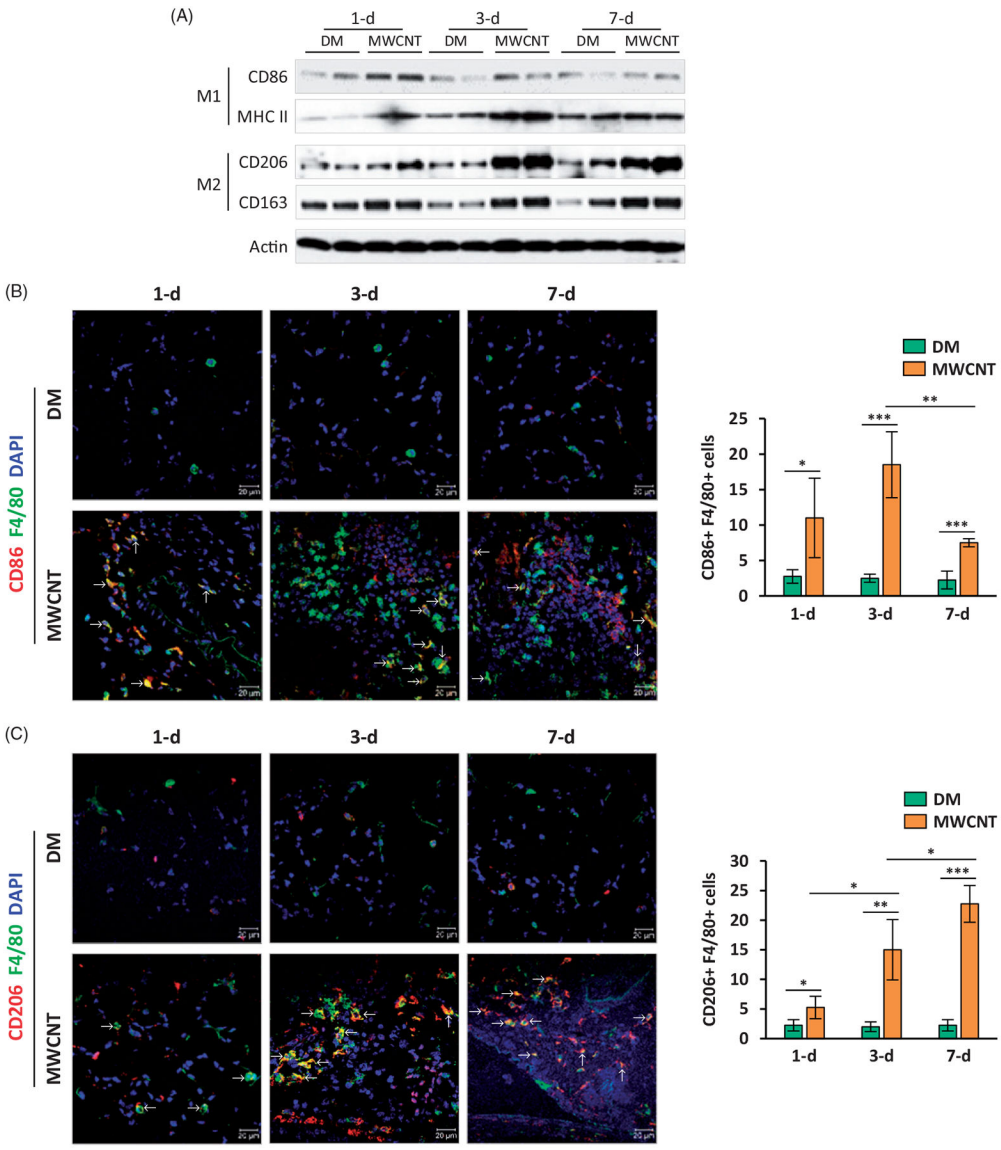

Figure 2.

M1–M2 macrophage polarization. Wild-type mice treated with DM or MWCNTs (40 μg per mouse) were sacrificed on day 1, 3, or 7 post-exposure. (A) Immunoblotting. Macrophage surface proteins CD86 and MHC II were detected as markers for M1 macrophages, and CD206 and CD163 for M2 macrophages ($n = 2$). (B) M1 polarization examined by double immunofluorescence staining of CD86 (red) and F4/80 (green). (C) M2 polarization examined by double immunofluorescence staining of CD206 (red) and F4/80 (green). Blue indicates nuclear staining (scale bar: 20 μm). Representative double positive cells are marked with arrows. Quantification of double positive cells is shown as mean ± SD ($n = 4$).

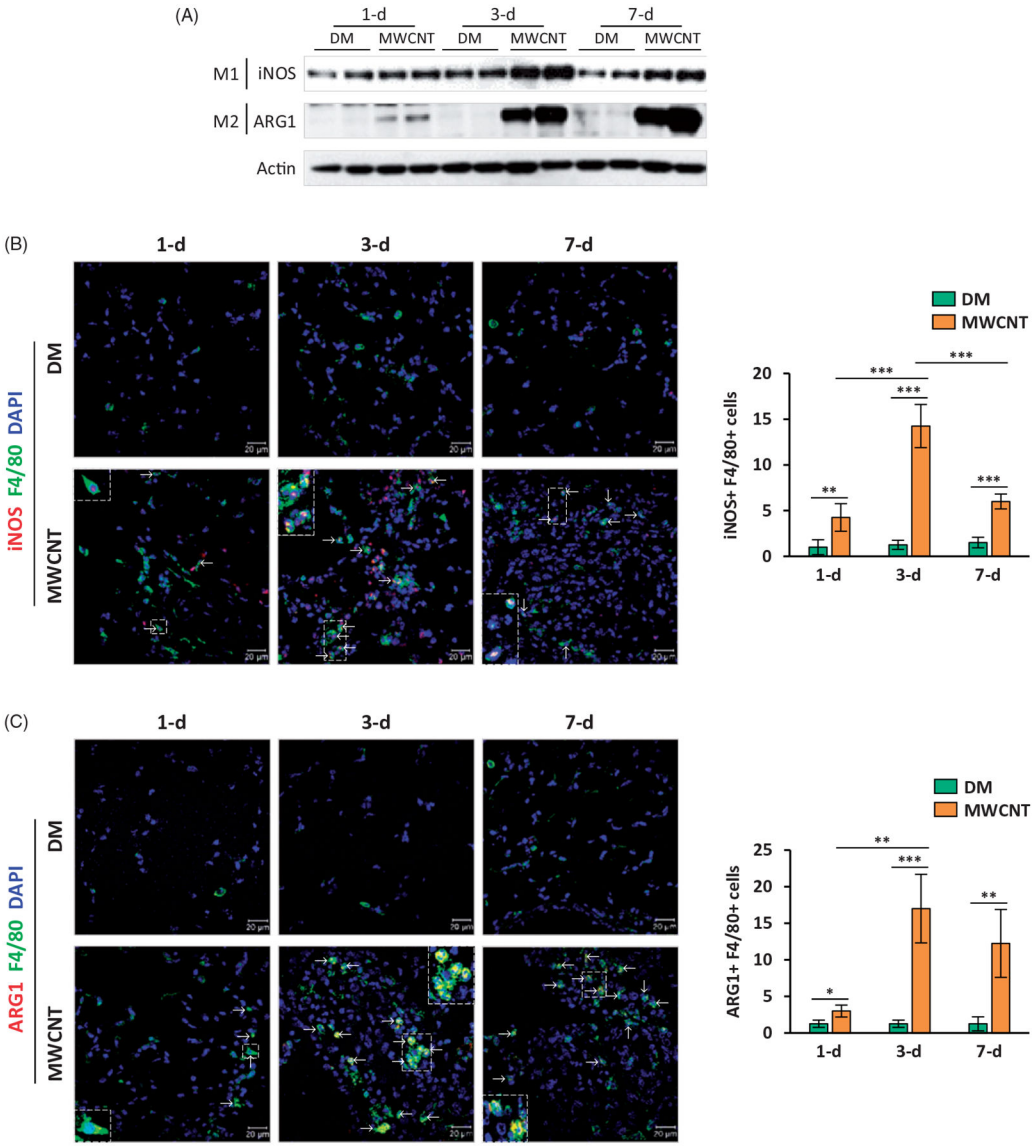

Figure 3.

Activation of M1 and M2 macrophages. Wild-type mice were exposed to DM or 40 μg MWCNTs for 1, 3, or 7 days. (A) Immunoblotting. iNOS was detected as a functional marker for M1 macrophage activation and ARG1 for M2 macrophage activation ($n = 2$). (B) M1 activation examined by double immunofluorescence staining of iNOS (red) and F4/80 (green). (C) M2 activation examined by double immunofluorescence staining of ARG1 (red) and F4/80 (green). Blue indicates nuclear staining (scale bar: 20 μm). Representative double positive cells are marked with arrows. Quantification of double positive cells is shown as mean ± SD ($n = 4$).

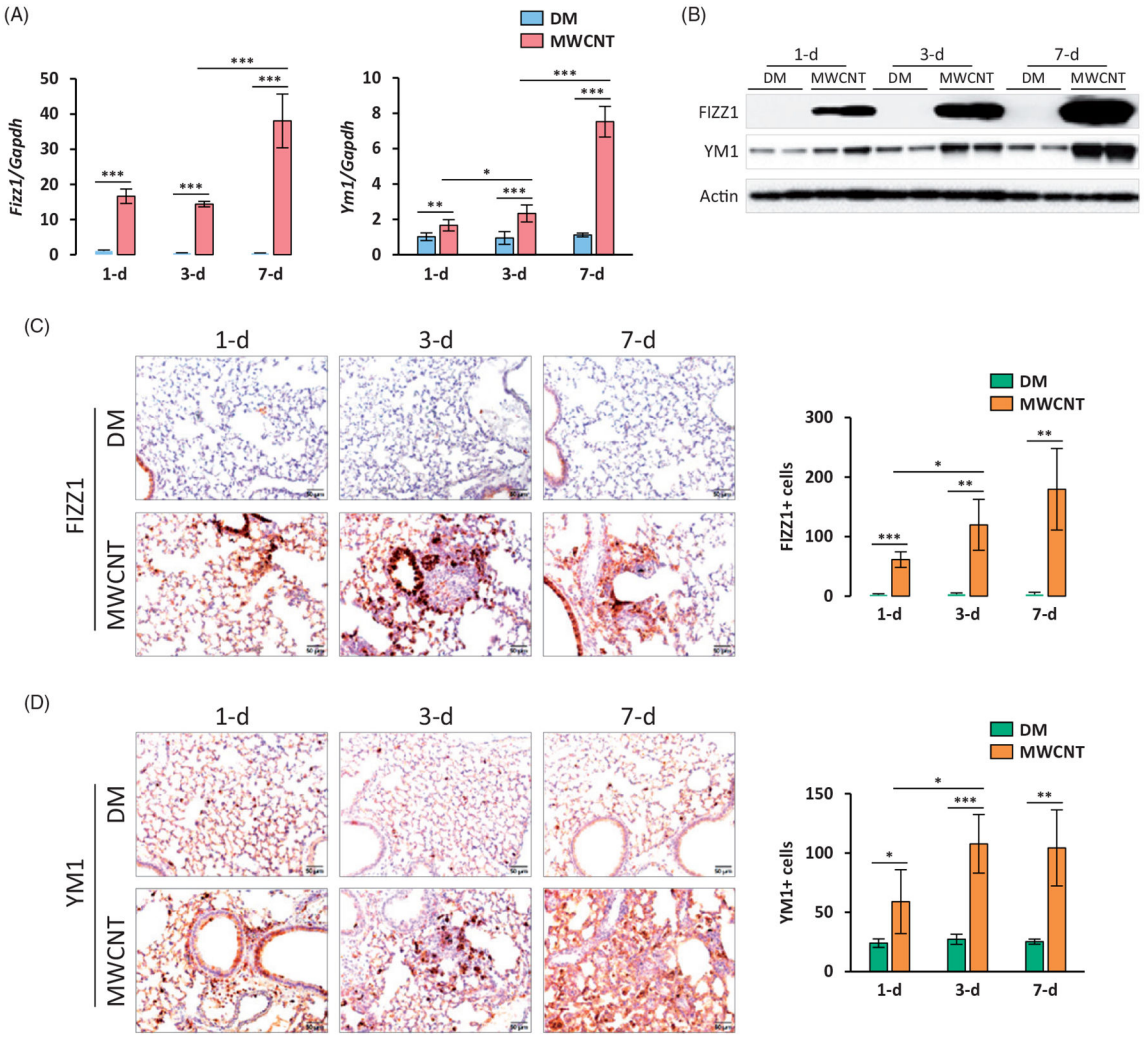

Figure 4.

Induction of FIZZ1 and YM1. Wild-type mice received DM or MWCNTs (40 μg per mouse) and were sacrificed on day 1, 3, or 7 post-exposure. (A) qRT-PCR. Levels of Fizz1 and Ym1 mRNA from lung tissues were determined, with Gapdh as internal control (mean ± SD, n = 5). (B) Immunoblotting. Levels of FIZZ1 and YM1 proteins in lung tissue lysates were determined (n = 2). (C) and (D) Time-dependent induction of FIZZ1 (C) and YM1 (D) detected by immunohistochemistry on lung tissue sections. Red indicates positive staining and blue nuclear counterstaining (scale bar: 50 μm). Quantification of positively stained cells is shown as mean ± SD (n = 4).

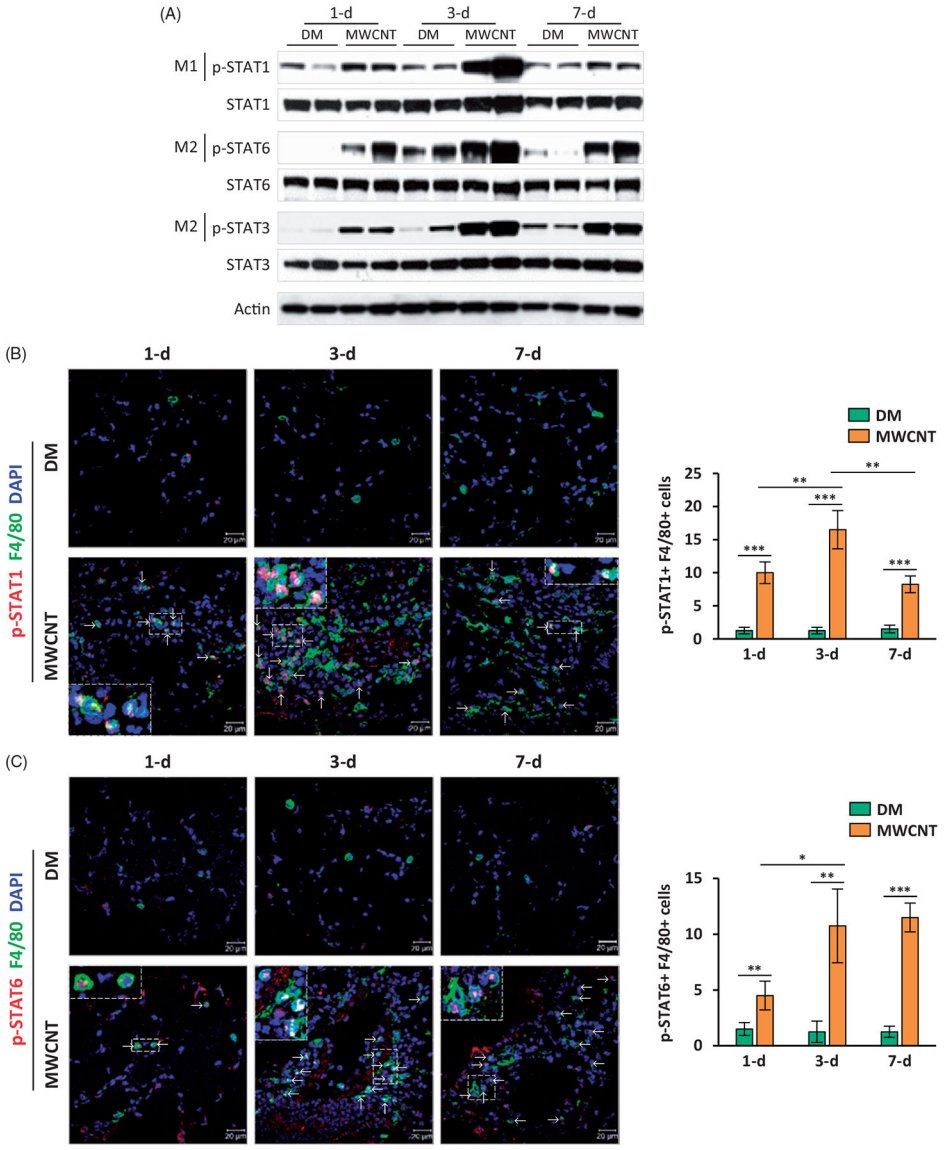

Figure 5.

Activation of STAT signaling. Wild-type mice were exposed to DM or 40 μg MWCNTs for 1, 3, or 7 days. (A) Immunoblotting. Phosphorylated STAT1 was detected as a marker for activation of M1 signaling, whereas phosphorylated STAT6 and phosphorylated STAT3 were examined for M2 signaling activation ($n = 2$). In addition to the Actin control, STAT1, STAT6, and STAT3 levels were examined as controls for the phosphorylated proteins, respectively. (B) Time-dependent activation of M1 signaling examined by double immunofluorescence staining of p-STAT1 (red) and F4/80 (green). (C) Time-dependent activation of M2 signaling determined by double immunofluorescence staining of p-STAT6 (red) and F4/80 (green). Blue indicates nuclear staining (scale bar: 20 μm). Representative double positive cells are marked with arrows. Quantification of double positive cells is shown as mean ± SD ($n = 4$).

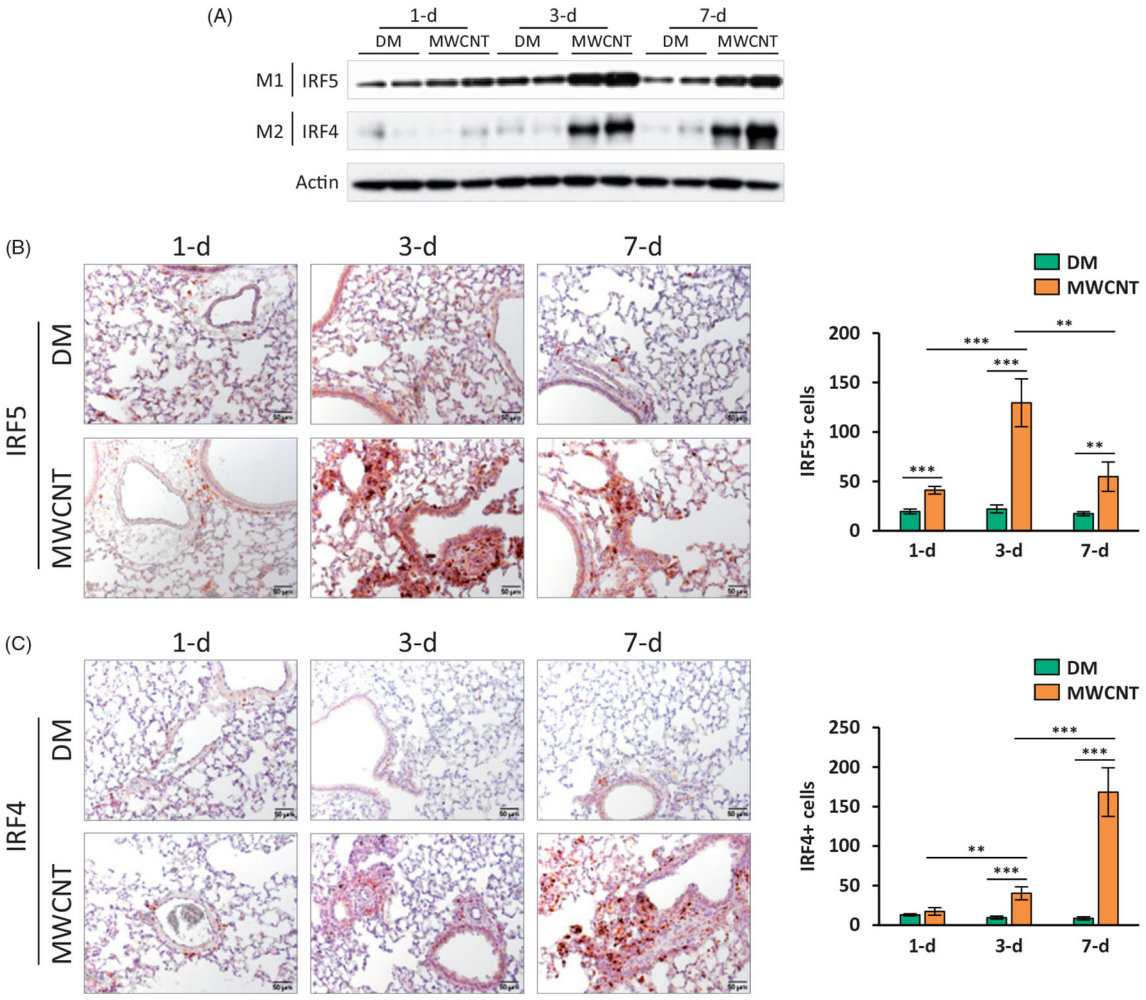

Figure 6.

Activation of IRF signaling. Wild-type mice received DM or MWCNTs (40 μg per mouse) and were sacrificed on day 1, 3, or 7 post-exposure. (A) Activation of IRF signaling examined by immunoblotting. IRF5 was detected as a marker for M1 signaling activation and IRF4 for M2 signaling activation ($n = 2$). (B) and (C) Time-dependent induction of IRF5 (B) and IRF4 (C) detected by immunohistochemistry. Red indicates positive staining and blue nuclear counterstaining (scale bar: 50 μm). Quantification of positively stained cells is shown as mean ± SD ($n = 4$).